Journal of
Ship&Ocean
Technology

SOTECH Vol. 9, No. 3, pp. 1 ~ 13, 2005

Development of an Optimal Hull Form with Minimum Resistance in Still Water

Hee-Jong Choi[1], Mun-Chan Kim[1] and Ho-Hwan Chun[1]

[1] Advanced Ship Engineering Research Center, Pusan National University, Busan, Korea
E-mial: choihj1988@hanmail.net

Abstract

A design procedure for a ship with minimum total resistance has been developed using a numerical optimization method called SQP (Sequential Quadratic Programming) to search for optimized hull form and CFD(Computational Fluid Dynamics) technique. The friction resistance is estimated using the ITTC 1957 model-ship correlation line formula and the wave making resistance is evaluated using a potential-flow panel method based on Rankine sources with nonlinear free surface boundary conditions. The geometry of hull surface is represented and modified using B-spline surface patches during the optimization process.

Using the Series 60 hull (C_B =0.60) as a base hull, the optimization procedure is applied to obtain an optimal hull that produces the minimum total resistance for the given constraints. To verify the validity of the result, the original model and the optimized model obtained by the optimization process have been built and tested in a towing tank. It is shown that the optimal hull obtained around 13% reduction in the total resistance and around 40% reduction in the residual resistance at a speed tested compared with that of the original one, demonstrating that the present optimization tool can be effectively used for efficient hull form designs.

Keywords: hull optimization, minimum total resistance, rankine source panel method, SQP(Sequential Quadratic Programming)

1 Introduction

Since the development of the landmark thin-ship theory of Michell(1898) considerable efforts to predict the ship resistance have been devoted toward the development of CFD(Computational Fluid Dynamics) techniques over a century. The robust and practical CFD technique has been developed in the past decades and it has been used as a replacement to the towing tank testing since a CFD technique has advantages compared with the towing tank testing in terms of cost reduction as well as quantities of detailed flow field information. Among CFD techniques, the potential-flow panel method based on Rankine sources with nonlinear free surface boundary conditions is preferable in ship yards because of its simplicity and the merits of computational cost in spite of its negligence of viscosity.

With the development of aforementioned CFD techniques and the improvement of computer performance the more comprehensive research to automatically modify the shape of hull form giving less resistance by CFD-based optimization technique has been only very recently performed and interest in the prediction of the optimal hull form at a given design constraint has been ever growing. Although some of these researches have given some encouraging results, there are still a number of nontrivial difficulties: selection of an appropriate objective function, choice of optimization scheme, geometric representation of hull surface and choice of a practical, robust CFD tool to evaluate the objective function and the large computational cost to estimate the objective function through the repeated calculations during the whole optimization process.

Recently many interesting papers on the hull form optimization from a resistance point of view have been published. Tahara et al(1998) developed a ship optimization method using the RANSE solver and SQP algorithm and performed hull optimization for Model 5415 hull and showed the optimized hull form. Hino et al(1998) also developed a ship optimization method using Navier-Stokes solver and SQP algorithm. Peri et al(2001) presented several new optimized bulb shapes for a tanker with the aid of the potential flow solver using linearized free surface conditions and three different optimization algorithm(Conjugate Gradient, Steepest Descent and SQP), showing a verification by comparing with the experiments. Markov et al(2001) performed optimization for Series 60 hull and HTC (Hamburg Test Case) containership using a higher-order Rankine source panel method to evaluate the wave resistance and DFP(unconstrained Davidson-Fletcher-Powell) as a optimization method and used a B-spline patch to approximate the hull surface during the optimization process. Choi et al(2003) developed a ship optimization method using the potential-flow panel method based on Rankine sources with nonlinear free surface boundary conditions and SQP method as a optimization technique and performed for KCS(KRISO Container Ship) and Series 60(C_B=0.6) hull.

In this paper, an optimization procedure for a ship with minimum total resistance is stated. To predict the total resistance as an objective function, the friction resistance is estimated using the ITTC 1957 model-ship correlation line formula and the wave resistance is evaluated using a potential-flow panel method based on Rankine sources with nonlinear free surface boundary conditions where the sinkage and trim of the ship are fully taken into account. The geometry of hull surface is represented and modified using non-uniform B-spline surface patches during the optimization process in which the B-spline coefficients are considered as the design parameters for the optimization.

To verify the validity of the optimization procedure, numerical computations are carried out for the Series 60 hull(C_B =0.60), and the original model and the optimized model obtained after the optimization process have been built and tested in the PNU(Pusan National University) towing tank.

2 Optimization Algorithm

2.1 General optimization problem

The general optimization problem may be expressed in the following form:

Minimize:

$$f(x) \tag{1}$$

Subjected to:

$$g_j(x)=0, \qquad j=1,\cdots,m_e \tag{2}$$

$$g_j(x) \le 0, \qquad j = m_e + 1, \cdots, m \tag{3}$$
$$x_l \le x \le x_u$$

where f is an objective function, g constraint functions, x the vector of the design variables, x_l and x_u lower and upper limit of x, m the number of constraint functions and m_e the number of equality constraint functions.

2.2 Nonlinear Programming Algorithm

In the present study, equation (1) and (2) are solved by sequential quadratic programming algorithm, in which the equations are approximated in quadratic form:

Minimize:

$$\frac{1}{2} d^T B d + \nabla f(x)^T d \tag{4}$$

Subjected to:

$$\nabla g_j(x)^T d + g_j(x) = 0, \qquad j = 1, \cdots, m_e$$
$$\nabla g_j(x)^T d + g_j(x) \ge 0, \qquad j = m_e + 1, \cdots, m \tag{5}$$

where d is search direction vector and B approximate Hessian matrix of the Lagrangian. During the optimization process optimum d is determined and x is updated by $x^{n+1} = x^n + d$ in each iteration(Vanderplaats 1984).

3 Objective function and evaluation

3.1 Potential-based Panel Method

Define a Cartesian coordinates system fixed on the ship which translates with a constant speed U and the x-axis points downstream and the z-axis upwards. In this frame of reference the vessel is stationary experiencing an incoming uniform stream U along the positive x-direction.

The fluid is assumed incompressible and inviscid and the flow irrotational, governed by the velocity potential ϕ subject to Laplace's equation in the fluid domain.

$$\nabla^2 \phi = 0 \tag{6}$$

Over the wetted part of the hull surface the velocity potential must satisfy the hull boundary condition of no flow normal to the surface.

$$\phi_n = 0 \tag{7}$$

where n is the unit normal vector.

The radiation condition must be satisfied

$$\nabla \phi \to (U,0,0) \qquad \text{as} \qquad x^2 + y^2 + z^2 \to \infty \tag{8}$$

On the free surface the kinematic and the dynamic conditions must be satisfied as stated in the following equations

$$\phi_x \eta_x + \phi_x \eta_x + \phi_z = 0 \quad \text{on} \qquad z = \eta \tag{9}$$

$$\eta = \frac{1}{2g}\left(U^2 - \nabla\phi \cdot \nabla\phi\right) \tag{10}$$

Since equation (9) and (10) are fully nonlinear equations, in this paper the iteration procedure is used to solve the free surface problem based on the Rankine source panel method (Choi et al. 2001, Raven 1992, Raven 1993).
Having obtained the velocity potential and hence the flow velocity, the pressure coefficient at each panel can be found using Bernoulli's equation

$$C_p = 1 - \frac{\nabla\phi \cdot \nabla\phi}{U^2} - 2\frac{z}{Fn^2} \tag{11}$$

The wave-resistance coefficient C_W is hence given by the pressure integral over the wetted hull surface

$$C_W = -\frac{\int_S C_p n_x ds}{S} \tag{12}$$

The frictional resistance coefficient is given by the ITTC 1957 model-ship correlation line formula.

$$C_F = \frac{0.075}{\left(\log_{10} Rn - 2\right)^2} \tag{13}$$

where S is the wetted surface of the hull and local Reynolds number is used for each element, based on the local velocity.
Finally the total resistance coefficient is obtained as follows

$$C_T = C_W + (1 + k)C_F \tag{14}$$

where the form factor $(1 + k)$ is calculated using the empirical formula presented by Holtrop et al(1984).

4 Modification of hull geometry

4.1 B-spline surface modeling

In the implementation of an optimization procedure, it is essential to have an efficient algorithm for geometry modification. The modified geometry should meet original design requirements without discontinuities in the surface and should be generally as smooth as possible. For ship hull optimization, it is necessary to use factors which are related to hull geometry generation as design variables. In this case, the increase of design variables means the increase of computation time. If the number of design variables is too small, realistic geometry may not be obtained. These requirements have been obtained by using a B-spline patch:

$$Q(u,v)=\sum_{i=1}^{n_i+1}\sum_{j=1}^{n_j+1}B_{i,j}N_{i,k}(u)M_{j,l}(v) \tag{15}$$

where $B_{i,j}$'s are the vertices of a defining polygon net, $N_{i,j}(u)$ and $M_{i,j}(v)$ the B-spline basis function in the bi-parametric u and v directions, respectively. The definition for the basis functions is as follows

$$N_{i,k}(u)=\begin{cases}1 & \text{if } x_i \le u < x_{i+1}\\ 0 & \text{otherwise}\end{cases} \tag{16}$$

$$N_{i,k}(u)=\frac{(u-x_i)N_{i,k-1}(u)}{x_{i+k-1}-x_i}+\frac{(x_{i+k}-u)N_{i+1,k-1}(u)}{x_{i+k}-x_{k+1}} \tag{17}$$

and

$$M_{j,1}(v)=\begin{cases}1 & \text{if } y_j \le v < y_{i+1}\\ 0 & \text{otherwise}\end{cases} \tag{18}$$

$$M_{j,l}(v)=\frac{(v-y_j)M_{j,l-1}(v)}{y_{j+l-1}-y_j}+\frac{(y_{j+l}-v)M_{j+1,l-1}(v)}{y_{j+l}-y_{j+1}} \tag{19}$$

where the x_i and y_j are elements of knot vectors.

4.2 B-spline surface fitting

When the surface is described by external data, it is convenient to obtain an initial non-flat B-spline surface approximating the hull for subsequent real time interactive modification. This requires determining the defining polygon net from an existing network of three dimensional surface data points.

For each known surface data point equation (15) provides a linear equation in the unknown $B_{i,j}$'s and similarly for all the surface data points. In matrix notation this can be written as

$$[D]=[C][B] \tag{20}$$

where $C_{i,j}=N_{i,k}M_{j,l}$. For arbitrary $r*s$ topologically rectangular surface point data, $[D]$ is an $r*s\times 3$ matrix containing the three-dimensional coordinates of the surface point data, $[C]$ is an $r*s\times n*m$ matrix of the products of the B-spline basis functions, and $[B]$ is an $n*m\times 3$ matrix of the three-dimensional coordinates of the required polygon net points.

Since for any arbitrary $r*s$ topologically rectangular surface point data, $[C]$ is not normally square, a solution can only be obtained in some mean sense. In particular

$$[B]=\left[[C]^T[C]\right]^{-1}[C]^T[D] \tag{21}$$

The *u* and *v* parametric values for each surface data are obtained using a chord length approximation (Huang el al 1998, Rogers 1990).

5 Hull form optimization example

The method described above is applied to an optimization problem in which numerical calculation has been performed using the Series 60 hull (C_B=0.60) as a reference hull at a speed(Fn=0.316).

5.1 Design variables

Since the potential flow solver is used to calculate the wave making resistance as a part of the objective function, the panels which define the shape of the ship surface should be generated at each iteration step during the whole optimization process. To make the optimization algorithm more stable during the numerical calculation the representation of the ship needs to be sufficiently flexible and robust to permit hull-form modifications, while involving only a moderate number of unknowns is an important factor of hull-form optimization.

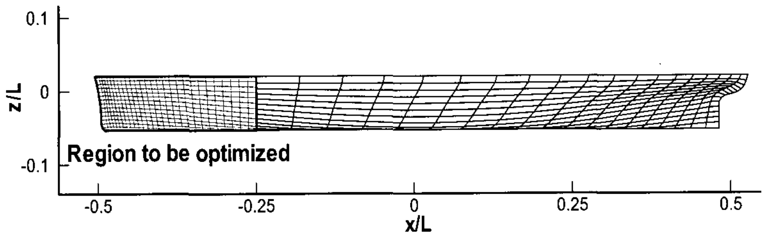

Figure 1: Region to be optimized

The ship surface is divided into 2 zones and the ship optimization is only performed to the region 25% from the bulb in which the flow is assumed to be potential flow as shown in Figure 1 Each zone is defined by a B-spline surface patch. In case of the region to be optimized a cubic surface with 10 by 7 control net (7 control points for each 10 section) is used to represent a ship form and the control vertices are used as design variables. The control vertices as design variables are repositioned according the optimization algorithm and used to generate the calculation panel for the flow calculation. For the other zone the control vertices are generated but not modified during the whole process and the same panel is generated for every iteration.

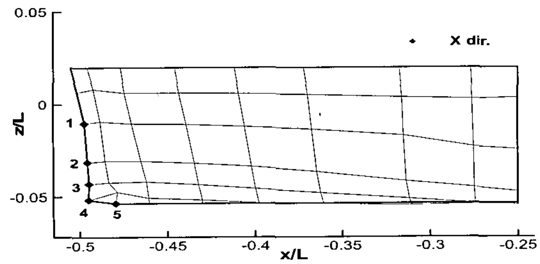

Figure 2: Design variables varying in x direction

Figure 2 shows the design variables which are allowed to move in x-direction. The design variables at the first and the second section have the same x-coordinates at each row to enforce continuity of curvature across the centerplane.

As the design variables move in x-direction the x-coordinates of the other control vertices between the second and the last section move in inverse proportion to the distance between the two points. To keep the reasonable ship shape the range of the movement of the control vertices is just confined as shown in Equation (22).

$$\begin{aligned} -0.5500 &< x_1 < -0.4972 \\ -0.5500 &< x_2 < -0.4955 \\ -0.5500 &< x_3 < -0.4947 \\ -0.5500 &< x_4 < -0.4949 \\ -0.5500 &< x_5 < -0.4749 \end{aligned} \tag{22}$$

Figure 3 shows the design variables which are allowed to move in y-direction. To keep the reasonable ship shape the range of the movement of the control vertices is just confined as shown in Equation (23).

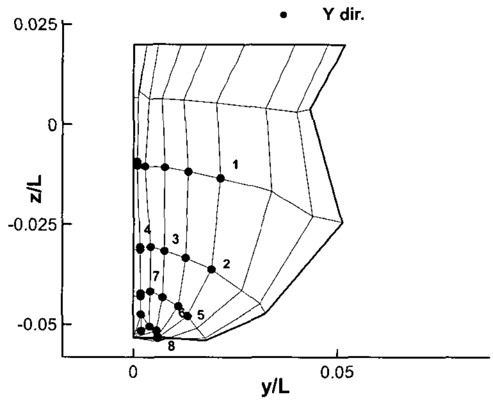

Figure 3: Design variables varying in y dir.

$$\begin{aligned} 0.0212 &< y_1 / L < 0.0300 \\ 0.0190 &< y_2 / L < 0.0300 \\ 0.0000 &< y_3 / L < 0.0160 \\ 0.0000 &< y_4 / L < 0.0100 \\ 0.0132 &< y_5 / L < 0.0300 \\ 0.0110 &< y_6 / L < 0.0300 \\ 0.0000 &< y_7 / L < 0.0140 \\ 0.0058 &< y_8 / L < 0.0060 \end{aligned} \tag{23}$$

The range of the movement for the other design variables to be allowed in y-direction is confined as follows

$$0.0000 < y / L < 0.0300 \tag{24}$$

5.2 Constraint conditions

The displacement and the wet surface area are most important factors from the total resistance point of view and hence, for the ship optimization process constraints of these values are pre-described, depending on the requirement of ship designer.
In this study the constraint for the displacement is set as follows, which may be a severe penalty from a resistance point of view.

$$\Delta \geq \Delta_{initial} \tag{25}$$

The normal vector is used to prevent the ship surface modifications which are undesirable.

$$n_x \leq 0 \tag{26}$$

$$n_y \geq 0 \tag{27}$$

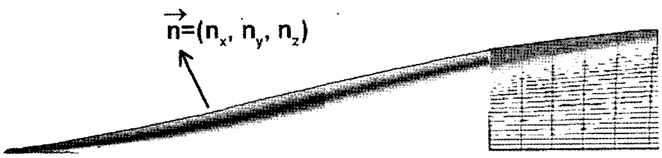

Figure 4: Definition of *n*

Equation (26) and (27) are important constraints since all numerical calculations during the optimization process are performed automatically so that the ship shape has a reasonable shape at every iteration without any external modification and it is known that the numerical calculation is more stable and the ship shape is modified in more smooth way by enforcing equations (26) and (27).

5.3 Computational results

Figure 5 shows the variation of R_T / R_T^0 with respect to the number of iteration.

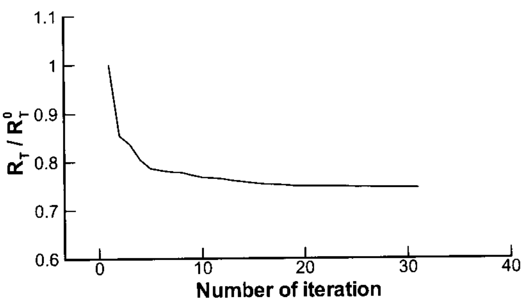

Figure 5: Convergence history

Here, R_T^0 is the total resistance for the initial hull form. This figure shows that the resistance is quickly reduced by first 5 iterations and the reduction rate is slowly decreased and finally converged.

It is seen from Figure 6 that the volume of the middle part of the fore body is increased dramatically and the fore body is bulb-shaped compared with that of the original one. Although aforementioned some constraints are provided to prevent an unusual hull form generation, it is still noticed that there are some unusual curves which seem to be not easily acceptable from a practical point of view.

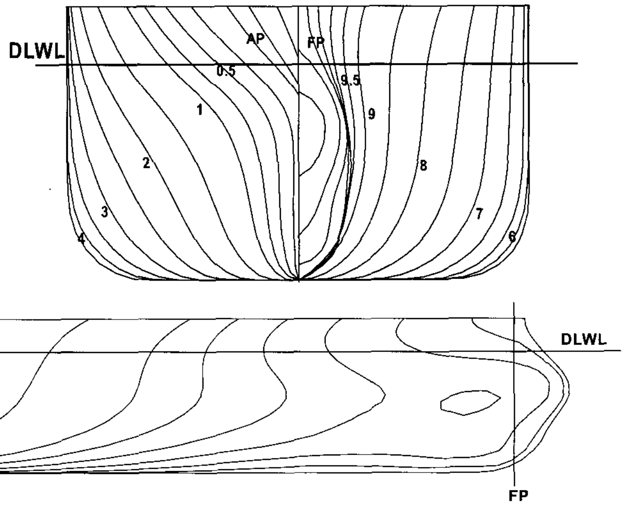

Figure 6: Optimal hull form after computation

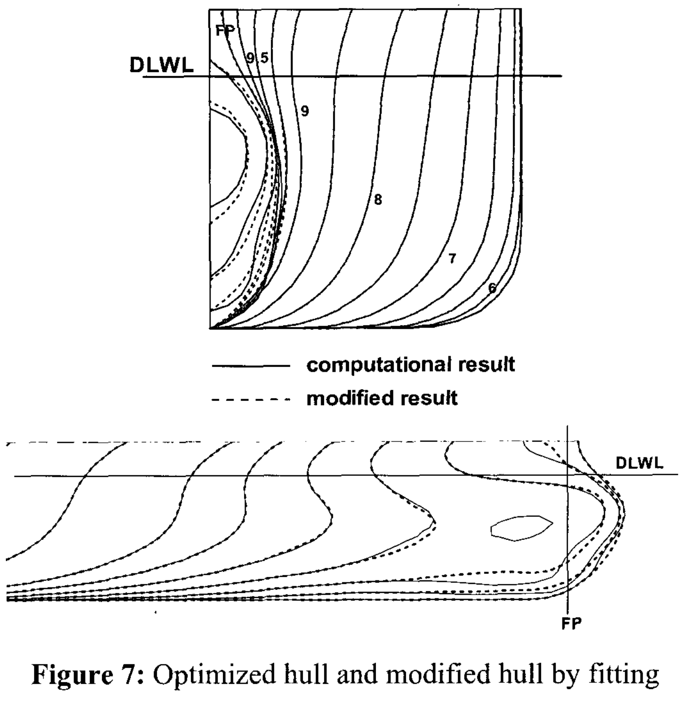

Figure 7: Optimized hull and modified hull by fitting

Then, the optimized hull is slightly modified by a fitting and Figure 7 shows the comparison between the original hull without modification and the final one after modification. In this modification a great care was taken to keep the main feature of the optimal hull.

To know the effect of the final modification numerical analysis is performed for the two hulls. This additional computation is to confirm that main features of the optimized hull were not changed and that the total resistance reduction was almost the same for the two hulls. Figure 8 and Figure 9 shows the comparison of the original Series 60 hull and the optimal hull form, clearly showing that the optimal hull has a big bulb whose resistance comparisons are shown later.

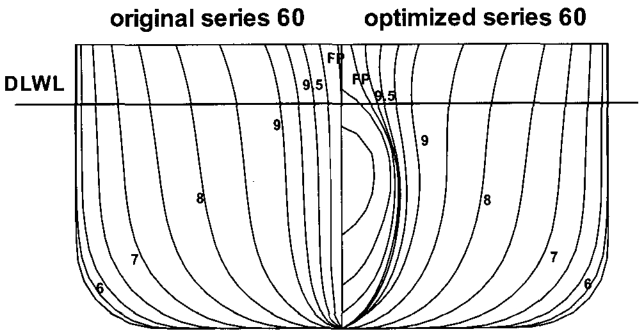

Figure 8: Comparisons of body plans for the original Series 60 and optimal hulls

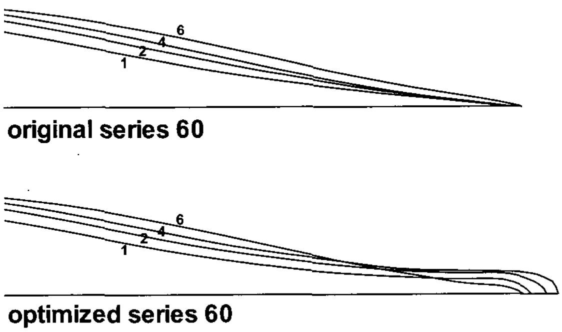

Figure 9: Comparisons of fore part waterlines for the original Series 60 and optimal hulls

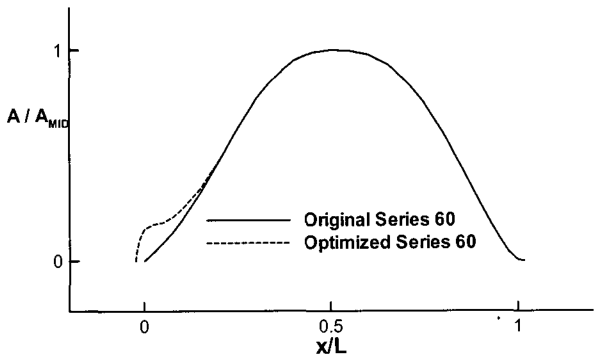

Figure 10: Comparison of sectional area curve for two hulls

Figure 10 illustrates the sectional area curve which shows a big volume increase in the fore part of the optimal hull.

The wave profile of a longitudinal wave cut close to the hull side is compared for the original and the optimized hull in Figure 11 where the experimental result for the original hull is shown for comparison. The wave amplitude on the fore-body part of the optimal hull is considerably reduced which explains the lower wave resistance due to the interference between of the hull and bow bulb. The whole wave system, as shown in Figure 12, is reduced as well.

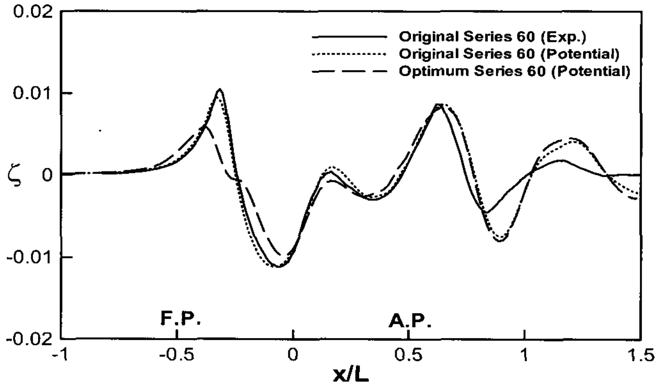

Figure 11: Wave profiles at y/Lpp=0.08 for Fn=0.316

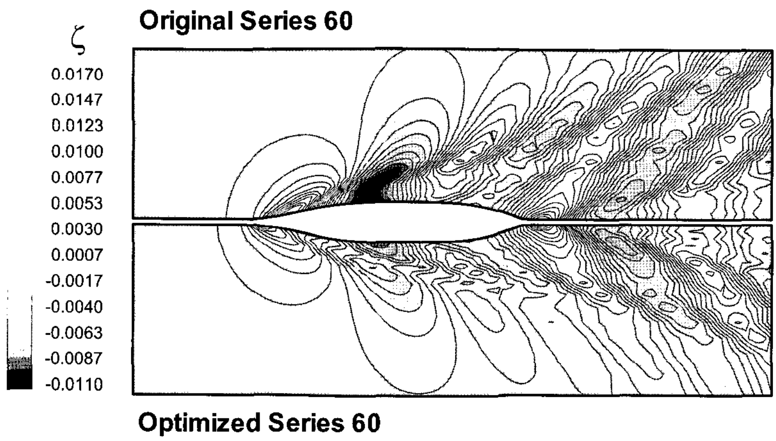

Figure 12: Wave patterns for Fn=0.316

5.4 Experimental validation

The model test was carried out for both the original and the optimal hull in the PNU towing tank and the model length was 3 meters.

As seen in Figure 13, the total resistance is significantly reduced at the speed of Fn=0.316(around 13.3% reduction in the measurement, as seen in Table 1), where the optimization was done, although the wetted area and total volume of the optimal hull are increased by 0.9% and 2% compared with those of the original hull, respectively, as shown in Table 1. It is interesting to note that the total resistance of the optimal hull becomes less than that of the original hull at speeds lower than Fn=0.27. This may be due to the facts of the increased wetted area and volume, and also of unfavorable wave interferences by the presence of the bulb for the optimal hull.

The calculated wave resistance coefficients and the measured residuary resistance coefficients for the two hulls are shown in Figure14. It can be seen that the patterns of the calculated and measured values are similar to each other, but some quantitative discrepancy exists between the computation and measurements. This discrepancy may be due to the facts of numerical and experimental uncertainty errors (experimental uncertainty is estimated as an overall uncertainty of 2 % at Fn=0.316, including the bias and random errors, with slightly increased values at lower speeds). The main source of the numerical error may be from the neglect of viscosity and another source may be from the panel sensitivity and the free surface domain considered. The panel sensitivity error can be reduced by increasing the panel number, being large enough to obtain the converged value, and also the free surface domain should be large enough to have fully developed wave systems. After many numerical trials, these kind of errors were reduced to be minimal by increasing the panel number and extending the free surface domain as necessary.

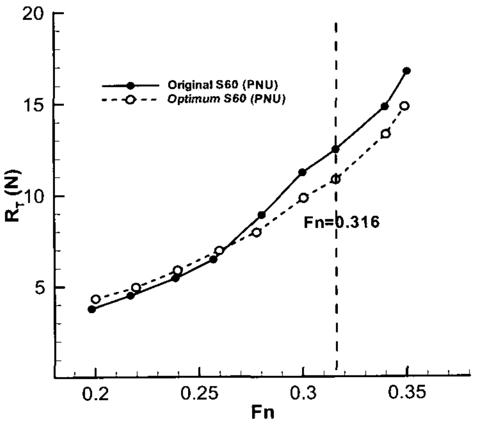

Figure 13: Comparison of R_T

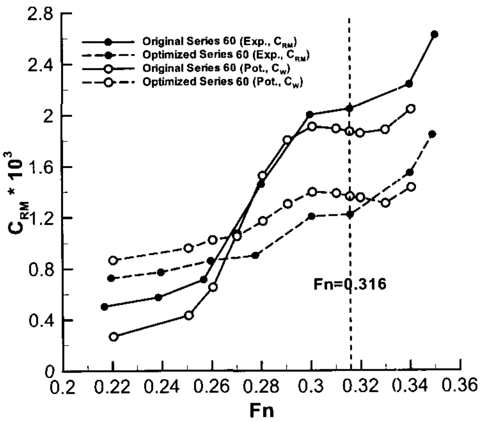

Figure 14: Comparison of $C_{RM}(C_{RW})$

As seen in Table. 1, the experimental results show that the residuary resistance of the optimal hull is reduced by 39.1% while the computational result shows 26.5% reduction. Nevertheless, the present optimization result with the potential code shows a right direction for improving hull form and accordingly, this tool can be effectively used for hull form design.

Table 1: Comparison of hydrostatic and hydrodynamic data for the two hulls at Fn=0.316

	Hull	*Original*	*Optimal*	*△(%)*
	∇	0.115	0.117	2.030
	S_{WET}	1.539	1.553	0.880
Potential flow Analysis	C_W (10^{-3})	1.860	1.360	-27.10
	R_W (N)	0.156	0.115	-26.50
Measured Data	C_{RM} (10^{-3})	2.040	1.220	-40.50
	R_{RM} (N)	4.620	2.820	-39.10
	R_{TM} (N)	12.48	10.83	-13.30

6 Conclusions

An optimization algorithm is developed to use hull form designs, using a potential panel code with nonlinear free surface boundary conditions where the sinkage and trim are fully taken into account, and this is tested and validated by comparing with the experiment. It is shown by the experiment that the optimal hull obtained using Series 60 (C_B =0.60) as a base ship gave 13 % reduction in the total resistance and 40% reduction in the residuary resistance. It should be noticed that this reduction rate mostly depend on choosing a base ship. For example, if the base hull with good resistance characteristics is chosen, the drag reduction rate for the optimal hull could be very less or even no achievement.

However, as demonstrated in the paper, this optimization tool can be effectively used to design a new hull form. In addition, this tool can be effectively used to improve hull forms by an experienced ship designer.

Acknowledgements

This work was supported by ASERC(Advanced Ship Research Center) of Pusan National University.

References

Choi, H.-J. and H.-H. Chun. 2001. Potential flow analysis for a hull with the transom Stern. J. of KCORE, **15**, **1**, pp. 1-6.

Choi, H.-J., K.-C. Seo, B.-E. Kim and H.-H. Chun. 2003. Development of an optimum hull form for a container ship with minimum wave resistance. J. of SNAK, **40**, **5**, pp. 8-15.

Hino, T., Y. Kodama and N. Hirata. 1998. Hydrodynamic shape optimization of ship hull forms using CFD. 3rd Osaka Colloquium on Advanced CFD Applications to Ship Flow and Hull Form Design, 332-340.

Holtrop, I.J. 1984. A statistical re-analysis of resistance and propulsion data. International Ship-Building Progress, **31**, 272-276.

Huang, C.H., C.C. Chiang, and S.K. Chou. 1998. An inverse geometry design problem in optimizing hull surfaces. J. of Ship Research, **42**, **20**, 79-85.

Markov, N.E. and K. Suzuki. 2001. Hull form optimization by shift and deformation of ship sections. J. of Ship Research, **45**, **3**, 197-204.

Michell, J.H. 1898. The wave resistance of a ship. Philosophical Magazine, **5**, **45**, 106-122.

Peri, D., M. Rosetti and E.F. Campana. 2001. Design optimization of ship hulls via CFD techniques, J. of Ship Research, **45**, **2**, 140-149.

Raven, H.C. 1992. A practical nonlinear method for calculating ship wavemaking and wave resistance. 19th Symposium on Naval Hydrodynamics, Seoul.

Raven, H.C. 1993. Nonlinear ship wave calculation using the RAPID method. 6th International Conference on Numerical Ship Hydrodynamics.

Rogers, D.F. and J.A. Adams. 1990. Mathematical Elements for Computer Graphics. McGraw-Hill, New York.

Tahara, Y., Y. Himeno. 1998. An application of computational fluid dynamics to tanker hull form optimization problem. 3rd Osaka Colloquium on Advanced CFD Applications to Ship Flow and Hull Form Design, Osaka Prefecture Univ. and Osaka Univ., Japan.

Vanderplaats, G.N. 1984. Numerical Optimization Techniques for Engineering Designs. McGrow-Hill, New York.